Polyelectrolyte–surfactant complex: phases of self-assembled structures

C. von Ferber*[a] and H. Löwen[b]

[a] *Theoretical Polymer Physics, Freiburg University, 79104, Freiburg, Germany. E-mail: ferber@physik.uni-freiburg.de*

[b] *Institut für Theoretische Physik II, Heinrich-Heine-Universität Düsseldorf, 40225, Düsseldorf, Germany*

Received 29th March 2004, Accepted 28th April 2004
First published as an Advance Article on the web 27th September 2004

We study the structure of complexes formed between ionic surfactants (SF) and a single oppositely charged polyelectrolyte (PE) chain. For our computer simulation we use the "primitive" electrolyte model: while the polyelectrolyte is modeled by a tethered chain of charged hard sphere beads, the surfactant molecules consist of a single charged head bead tethered to a tail of tethered hard spheres. A hydrophobic attraction between the tail beads is introduced by assuming a Lennard-Jones potential outside the hard-sphere diameter. As a function of the strengths of both the electrostatic and the hydrophobic interactions, we find the following scenario: switching on and increasing the electrostatic forces first leads to a stretching of the PE and then by condensation of SF to the formation of a complex. For vanishing hydrophobic forces this complex has the architecture of a molecular bottle-brush cylindrically centered around the stretched PE molecule. Upon increasing the hydrophobic attraction between the SF tails, a transition occurs inverting this structure to a spherical micelle with a neutral core of SF tails and a charged corona of SF heads with the PE molecule wrapped around. At intermediate hydrophobicity there is a competition between the two structures indicated by a non-monotonic dependence of the shape as function of the Coulomb strength, favoring the cylindrical shape for weak and the spherical micellar complex for strong interaction.

I. Introduction

Polyelectrolyte–surfactant mixtures have proven to provide the basis for new materials with extraordinary properties that make them interesting for a wide range of applications.[1,2] In particular the Coulomb attraction between polyelectrolyte chains and oppositely charged ionic surfactant molecules in solution leads to aggregation and complex formation. The resulting complex differs in its conformational, structural and dynamical features from that of a solution containing only one of its constituents, the pure polyelectrolyte or the pure surfactant (for reviews see ref. 1 and 3). Much experimental work has been done on these systems and a rich variety of different complex structures was revealed as a function of chemical nature of the polyelectrolyte, surfactant and solvent molecules.[4–15] A theory that could give a systematic microscopic characterization and prediction of the different complexes on the other hand does not exist so far.

For complexes formed by a *single* polyelectrolyte chain with ionic and hydrophobic surfactants at low concentration a theoretical treatment that takes the long-ranged Coulomb interaction and the

hydrophobic interactions fully into account is still to be developed. The case without hydrophobicity has recently been simulated by the present authors.[16] For these single polyelectrolyte complexes one expects structures either of bottle-brush shape for low hydrophobicity or, for strong hydrophobicity, possibly spherical micelles that aggregate together with the polyelectrolyte chain.[2,17] Theories so far in general make assumptions about the symmetry or the structure of the complex implying a complete adsorption of surfactant onto the polyelectrolytes for rigid[18,19] and flexible chains, see *e.g.* ref. 20, and cannot predict the complex structure or its symmetry[17] as far as it enters the theory as an input. For the special case of a system of rigid polyelectrolytes that form complexes *via* thermodynamic counterion condensation including the effect of added surfactant a theory has recently been developed by Kuhn, Levin and coworkers.[21–23] The collapse and partial collapse of semiflexible and flexible polymers in solutions with surfactants has been treated by a meanfield association theory by Diamant and Andelman.[24,25] However, this theory does not include explicitly the long range of the Coulomb interactions. A self consistent field theory with a spherically symmetric setup[17] on the other hand predicts the formation of spherically symmetric micelles with a neutral hydrophobic core and a surface layer where the charged surfactant heads and the oppositely charged polyelectrolyte are located. Based on this observation it has been proposed to simplify the model by replacing the ionic surfactant by large spherical counterions not treating the surfactant tails explicitly.[26] For a system of a polyelectrolyte in the presence of small counterions computer simulations[27–29] and theories[30,31] find a swelling and stretching of the polyelectrolyte and a subsequent collapse when increasing the Coulomb interaction. In this scenario a non-monotonic dependence of the polyelectrolyte conformation as a function of the Coulomb strength occurs: for weak Coulomb strength the PE stretches while in the strong Coulomb regime counterion condensation and a collapse to a coil conformation occurs. For large counterions representing micelles the polyelectrolyte may be wrapped around the charged sphere exhibiting different conformations depending on the chain flexibility.[26,32–46]

The bottle brush structure that is expected for the condensation of charged ionic surfactants onto a polyelectrolyte chain may be compared with corresponding neutral molecular bottle brushes in case the polarization effects in the complex are neglected. Such neutral bottle brush or comb polymers are built either by end linking the side chains to the backbone chain or by attaching them *via* strong hydrogen bonds.[47,48] Such configurations may be expected to become more rigid for higher densities of the side chains. A quantitative description, however, is still under debate since different simple scaling arguments[49–51] appear to predict different quantitative behavior for the sizes of the main and side chains depending on the model used and the limit that is considered.[52]

In the present paper we explore by computer simulation the phases of complex formation of a single polyelectrolyte chain with ionic surfactants in the phase space parameterized by the strengths of the Coulombic interactions and the hydrophobic attraction between the surfactant tails. As in our previous study[16] our simulation relies on the so-called ''primitive'' model[53] that treats the microscopic charges of the polyelectrolyte and the surfactant heads explicitly. This is in contrast to simulations on polymer–surfactant complexation which neglect the long-range nature of the Coulomb interactions.[54] The ''primitive'' model has recently also been applied to simulate the complexation of polyelectrolyte chains with charged spheres representing spherical micelles[55] and has proven to be reliable in different contexts of polyelectrolyte conformations.[27–29,56–59]

To treat surfactants with neutral or hydrophobic tails we model the surfactant by a tethered hard sphere chain with a charged head and a Lennard-Jones like effective attraction between the hydrophobic tail monomers allowing for the formation of micelles. As a result, we observe different phases of complexation depending on the strengths of the two interactions involved: the Coulomb and the hydrophobic interaction. An overview of these phases is given in Fig. 1 in terms of simulation snapshots. For vanishing hydrophobicity (leftmost column of Fig. 1) the mean square end–end distance R^2 of the polyelectrolyte is non-monotonic as a function of the Coulomb interaction. However, in contrast to the standard situation where a collapse of the polyelectrolyte due to counterion condensation occurs,[27–29] such a collapse is blocked by the steric interaction of the surfactant tails. As we have shown in ref. 16, for even longer surfactant tails the collapse is more sufficiently blocked, while the addition of salt weakens the complex as it replaces the surfactant in the complex. Increasing the hydrophobicity for vanishing Coulomb interaction on the other hand (bottom row of Fig. 1) leads to the aggregation of micellar clusters of surfactant molecules that are independent from the polyelectrolyte chain. Introducing a finite Coulomb strength in this latter

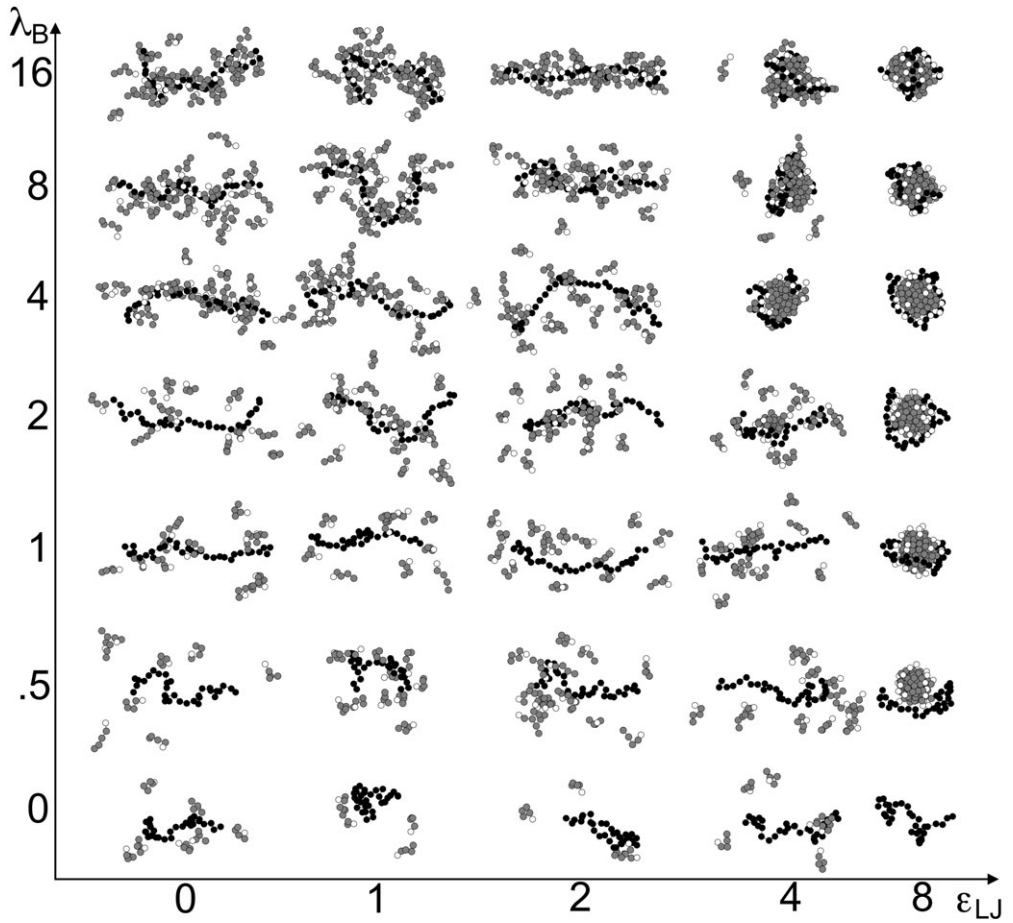

Fig. 1 Snapshots of the complex configurations showing the dependence on the two interactions: Coulombic (λ_B) and hydrophobic (ε_{LJ}).

situation favors the condensation of the surfactant at the polyelectrolyte. Thirdly we may start with a bottle brush conformation of the complex at high Coulomb but vanishing hydrophobic interactions (top left of Fig. 1). Gradually increasing the hydrophobicity (along the top row of Fig. 1) the tails start to aggregate and a transition occurs from the cylindrical structure with the tails on the outside to an inverted spherical structure with a core that is constituted by the surfactant tails. In our present resolution this transition appears to be sharp.

The paper is organized as follows: in section II, we describe our model in detail and we present details of the simulation procedure in section III. Results are given in section IV and we conclude in section V.

II. The model

In our simulation we model all molecules as chains of tethered hard spheres (beads) that represent Kuhnian segments of the molecule. Microions are modeled by hard sphere beads. Charges on these molecules and ions are represented by placing a point charges at the center of any charged bead. In this primitive model the solvent is not treated explicitly and only enters *via* its dielectric constant ε_r neglecting the discreteness of the solvent molecules. The microscopic interactions between the particles are given by the hard sphere excluded volume, the long-ranged Coulomb forces, and a short range hydrophobic interaction. We reduce the model parameter space by fixing the hard

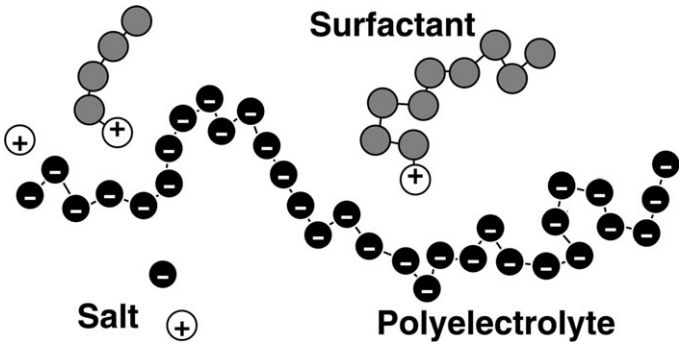

Fig. 2 Model of the polyelectrolyte–surfactant system with salt ions. Charges are indicated by "+" and "−" signs.

sphere diameter of all beads in the system to the same value σ. Furthermore, all charged beads have the same charge $\pm qe$ with e denoting the elementary charge. While this "minimal" model explicitly handles the counter ions and may be used to describe strongly charged, flexible polyelectrolytes,[27] analytical calculations usually neglect the individual character of the counter ions.[60–63]

As mentioned above, all molecules are modeled by chains of freely jointed, tethered hard sphere beads. Subsequent beads in the same chain are tethered. The extension of all bonds is limited by the tether to a fixed value b. For vanishing Coulomb and hydrophobic interactions the model is purely entropic (*i.e.* temperature-independent). Our specific parameters are such that the polyelectrolyte is represented by a chain of N charged beads each with charge $-qe$. The surfactant molecules on the other hand are chains of n tethered beads with one charged head bead of charge $+qe$ and $n-1$ neutral tail beads that may interact due to hydrophobicity. The full model may also contain salt which has been treated in ref. 16. The salt ions are then represented by single charged beads. The constituents of the model of polyelectrolytes, surfactant molecules and microions is schematically shown in Fig. 2.

In our model, the effective interaction due to hydrophobicity of the surfactant tails is given by a Lennard-Jones like potential between the tail monomers. This approach has also been used in the context of copolymer micellization.[64,65] The explicit interaction between any two beads i, j of the model at a distance r between their centers is given by a potential $V_{ij}(r)$. To denote chain connectivity we use an adjacency matrix T_{ij}. For beads i, j that are tethered $T_{ij}=1$ otherwise $T_{ij}=0$. With $q_i \in \{\pm 1, 0\}$ denoting the charge and $u_i \in \{1, 0\}$ the hydrophobicity number of bead i, the potential $V_{ij}(r)$ is given by

$$\frac{1}{k_{\mathrm{B}}T}V_{ij}(r) = q_i q_j \lambda_{\mathrm{B}} \frac{\sigma}{r} + u_i u_j \varepsilon_{\mathrm{LJ}} \left(\left(\frac{\sigma}{r}\right)^{12} - \left(\frac{\sigma}{r}\right)^{6} \right) + V_{\mathrm{H}}(\sigma - r) + T_{ij} V_{\mathrm{H}}(r-b). \tag{1}$$

Here, the dimensionless Coulomb strength λ_{B} is the Bjerrum length measured in bead diameters σ. The Bjerrum length $\sigma\lambda_{\mathrm{B}} = q^2e^2/\varepsilon_r k_{\mathrm{B}}T$ sets the length scale where the Coulomb pair interaction is comparable to the thermal energy $k_{\mathrm{B}}T$. The dimensionless hydrophobicity parameter $\varepsilon_{\mathrm{LJ}}$ controls the depth of the Lennard-Jones potential. Furthermore, the hard core and tether interactions are represented by the one dimensional hard wall potential

$$V_{\mathrm{H}}(x) = \begin{cases} 0 & \text{if } x<0 \\ \infty & \text{else} \end{cases}. \tag{2}$$

We note that in our notation the product $T_{ij}V_{\mathrm{H}}(r-b)$ is defined to be zero if T_{ij} is zero.

The key parameters of our model are: the number N of charged monomers of the polyelectrolyte chain, the number $n-1$ of neutral beads of the surfactant tails, the parameters λ_{B} and $\varepsilon_{\mathrm{LJ}}$ which measure the strengths of the Coulomb and hydrophobic interactions and finally the relative salt concentration c_s. In the following we shall explore the parameter space in particular in the two variables λ_{B} and $\varepsilon_{\mathrm{LJ}}$ while keeping fixed the particle hard-core diameters, the microion charges q_i, the monomer number $N=32$ and the maximal tether length $b=1.5\sigma$ and in general also the salt

concentration $c_s = 0$ and the surfactant length $n = 5$. In our previous work[16] we also investigated the influence of surfactant tail variation as well as of finite salt concentration. A brief discussion of the corresponding results is also included in the following.

III. Simulation technique

We simulate by standard Monte Carlo (MC) methods a system of a single polyelectrolyte chain of N charged beads at finite concentration with polyelectrolyte charge density $\rho = N/L^3 = 0.001\sigma^{-3}$ which is kept fixed throughout all simulations. The finite concentration is taken into account by periodic boundary conditions of our finite cubic simulation box of length L and replicated images of the charges. Summations over the interactions with the periodic images are calculated by the Lekner sum method.[66] The Metropolis rates of the MC moves are determined by the interactions given by eqn. (1).

The relaxation of the system, especially in the fully assembled bottle brush configurations is very slow. This is also known from simulations of conventional bottle brush molecules.[52] To ensure sufficient relaxation we performed $\sim 5 \times 10^6$ attempted MC moves per particle at each state point. The acceptance ratio is roughly 0.8 in situations with an open structure. In the micellar cases however, caging occurs inside the densely packed core reducing the acceptance rate down to 0.3.

In all simulations the global charge of our system vanishes. We performed simulations for a system of a single polyelectrolyte chain together with $N = 32$ oppositely charged surfactant molecules. The case $n = 1$ of no tail beads at all serves as a natural reference for pure counter ions. Such a situation was already studied in ref. 27 and implemented in the frames of the present setup in ref. 16 for different Bjerrum lengths. Note, however, that chain connectivity was modeled differently in ref. 27 *via* a finite extension potential.

IV. Results

A. Zero hydrophobicity of the surfactant

In the case of vanishing hydrophobic interactions $\varepsilon_{LJ} = 0$ the surfactant tails interact only due to their steric repulsion. This special case was treated by the present authors in ref. 16 in detail, so we only recall some of the basic results. We first discuss the case of no added salt. As a reference situation serves the surfactant without tail, *i.e.* $n = 1$. The averaged square end-to-end distance R^2 of the polyelectrolyte chain is defined *via*

$$R^2 = \langle (\vec{R}_1 - \vec{R}_N)^2 \rangle \tag{3}$$

where $\langle \ldots \rangle$ denotes a statistical average and $\vec{R}_1$ and $\vec{R}_N$ are the actual positions of the two end-monomers of the polyelectrolyte.

R^2 is plotted as a function of Coulomb strength λ_B in Fig. 3. Here, the collapse scenario found in other simulations[27–29] and analytical treatments[67] is confirmed. This scenario for simple counterions is the following: At zero Bjerrum length $\lambda_B = 0$ the interaction is purely excluded volume and the chain attains a polymer coil configuration. Increasing λ_B the chain stretches due to the repulsion of its charged beads. For low λ_B the counterion screening is weak and stretching continues until $\sigma\lambda_B$ is of the order of the counterion diameter, *i.e.* $\lambda_B \simeq 1$. For larger $\lambda_B > 1$ the condensation of counterions induces a shrinking of the PE extension which for high λ_B may even become smaller than the neutral coil; an effect not yet seen in the range for λ_B that we simulated.

Substituting in the former system the counterions by charged surfactants with neutral tails the behavior as a function of the Coulomb strength λ_B changes in the following way: The PE chain stretches for increasing λ_B with the maximal extension attained for higher values of λ_B corresponding to the the larger effective diameter of the charged surfactant acting as a counterion. When counterion condensation occurs at higher λ_B the surfactant and the PE chain form a complex in which the surfactants aggregate with their heads near the PE chain and their tails pointing away from the PE chain in a manner resembling the structure of a molecular bottle brush. The subsequent collapse of the PE chain that is observed in the previous scenario now is effectively blocked due to the excluded volume interaction of the surfactant tails. The internal structure of this complex is discussed below. For the special case of vanishing hydrophobicity the influence of added salt on the

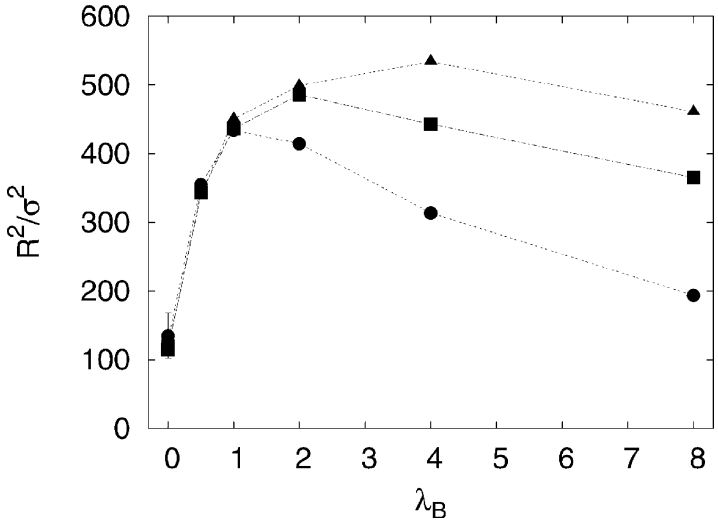

Fig. 3 The mean square end-to-end distance R^2 as a function of the Bjerrum length λ_B for $n = 1$(●), 5(■) and 10(▲) (from below) monomer surfactants for vanishing hydrophobicity parameter $\varepsilon_{LJ} = 0$. The statistical uncertainty is indicated by an error bar.

end-to-end distance R was investigated in ref. 16. Adding N_s additional 1 : 1 salt pairs to our system we define the relative concentration as $c_s = N_s/N$ where N is the number of charges on the polyelectrolyte. The results are shown in Fig. 4. The surfactant molecules in the complex are replaced in favor of salt ions. This is driven by entropy of mixing and corresponds to a chemical equilibrium. The replacement is therefore increasing with increasing salt concentration. This destroys the structure of the complex as seen from the reduction in the end-to-end distance of the polyelectrolyte.

In all our simulations we observe that the contour length L of the polyelectrolyte given by the sum of the bond lengths is very stable under all changes of the parameters. Varying the Bjerrum length in

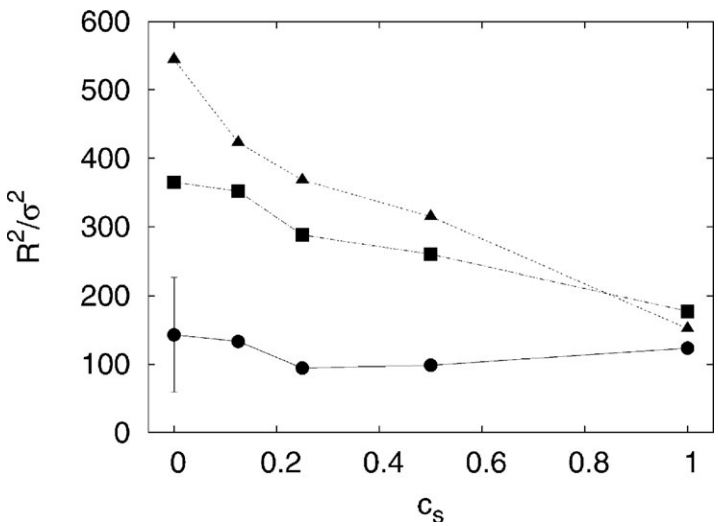

Fig. 4 The mean square end-to-end distance R^2 for Bjerrum length $\lambda_B = 8\sigma$ as a function of the relative salt concentration c_s for (from below) $n = 1$(●), 5(■) and 10(▲) monomer surfactants. The statistical uncertainty is indicated by an error bar.

the range $\lambda_B = 0...8$ we find a corresponding increase from $L = 40$ to $L = 42$, a change that is within the statistical uncertainty. For this reason also the persistence length L_p does not give additional information. For a worm-like chain namely it is related to the end–end distance R and the contour length L by[68]

$$R^2 = 2LL_p - 2L_p^2(1 - \exp(-L/L_p)) \tag{4}$$

a relation also confirmed by simulations.[27]

B. Clusters and micelles

The results described in this and the following sections all refer to a system with a single polyelectrolyte chain of 32 charged beads and 32 oppositely charged 5-bead surfactant molecules with one charged head bead and four neutral possibly hydrophobic tail beads. For finite values of the Coulombic and hydrophobic interactions we observe in general one or more aggregates or clusters of molecules. To analyze these structures in detail we define the clusters by assuming that any two beads belong to the same cluster if their distance is less than 2σ. Among these clusters we identify the complex as the one that contains the polyelectrolyte chain. We monitor the number of clusters and the sizes of the complex and of the largest aggregates that are detached from the polyelectrolyte. These latter aggregates we identify with isolated micelles. The number of identified clusters is shown in Fig. 5 as a function of the Coulomb interaction parameter λ_B for different values of the hydrophobicity strength ε_{LJ}: For vanishing interactions clustering occurs only by chance and almost each cluster observed represents one of the 33 single molecules in the system. For increasing interactions the molecules condense to a few larger clusters with only one or two remaining in the strong interaction case. When the Coulomb interaction vanishes, *i.e.* $\lambda_B = 0$, the polyelectrolyte will always be detached from the micelles and thus a minimal number of two clusters remain even for strong hydrophobic attraction. For any finite Coulomb interaction and high hydrophobicity on the other hand all molecules condense to a single complex in the present setup. The sizes of the complex and of the largest detached micelle are shown in Fig. 6 where we plot the masses of these aggregates as a function of the Coulomb parameter λ_B for different values of the hydrophobicity ε_{LJ}. It is clearly seen from these plots that a large detached micelle appears only for small Coulombic strength $\lambda_B < 1$ and high hydrophobic attraction $\varepsilon_{LJ} > 5$. For these high $\varepsilon_{LJ} > 4$ the largest detached micelle shrinks rapidly with increasing λ_B while at the same time the mass of the complex grows such that the surfactant is nearly quantitatively condensed in the complex for $\lambda_B > 1$. For smaller hydrophobicity $\varepsilon_{LJ} < 4$ on the other hand no larger detached micelles appear at all while the

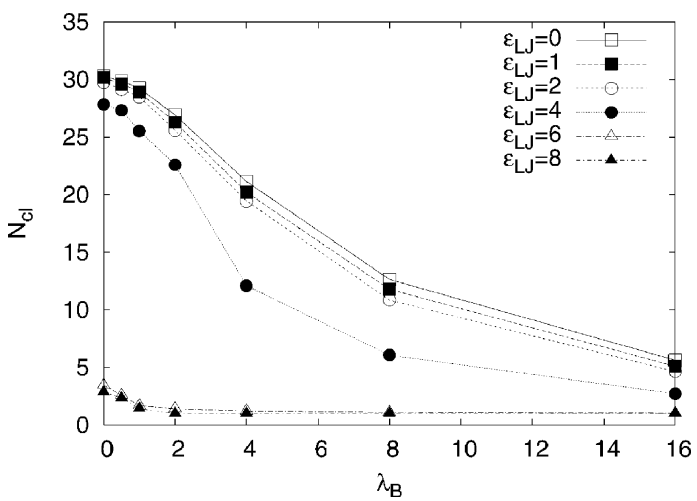

Fig. 5 The number of clusters N_{cl} in the system as function of the Coulomb strength λ_B for different values of the hydrophobicity parameter $\varepsilon_{LJ} = 0(\square), 1(\blacksquare), 2(\bigcirc), 4(\bullet), 6(\triangle), 8(\blacktriangle)$ from above.

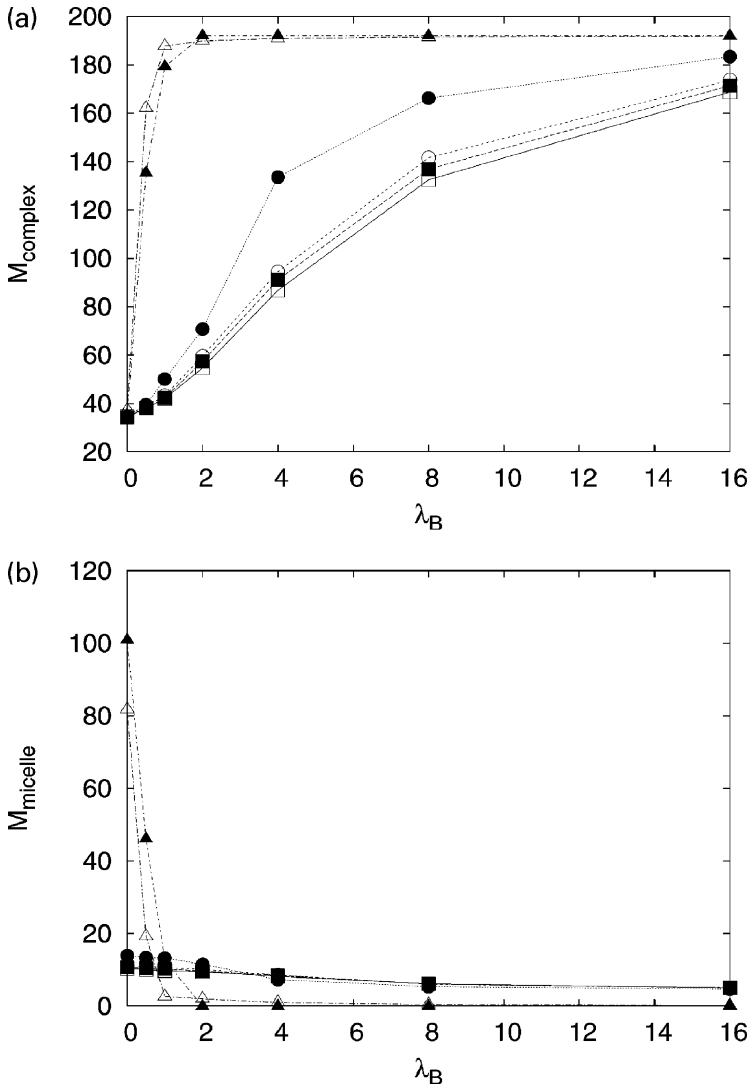

Fig. 6 (a) The total mass (number of beads) of the complex and (b) of the largest detached micelle as function of the Coulomb strength λ_B for different values of the hydrophobicity parameter $\varepsilon_{LJ} = 0(\square)$, $1(\blacksquare)$, $2(\bigcirc)$, $4(\bullet)$, $6(\triangle)$, $8(\blacktriangle)$ from above.

mass of the complex grows only moderately for increasing Coulombic strength λ_B. Thus, while for high hydrophobicity the size of the largest detached micelle is inversely related to the size of the complex, the absence of large micelles for smaller hydrophobicity may be explained with their instability due to the Coulombic repulsion between the charged surfactants in combination with entropy. As shown in the appendix the total binding energy of the surfactant tails in the micelle grows proportionally to its mass M_{mic} with a surface correction proportional to $M_{mic}^{2/3}$. The electrostatic energy of the surfactant heads on the other hand is proportional to $M_{mic}^{5/3}$ while the entropy term behaves like $M_{mic} ln\, M_{mic}$. The qualitative behavior of these three terms together with the approximate prefactors derived in the appendix may explain that for the finite number of available surfactants the formation of large detached micelles is unfavorable for $\varepsilon_{LJ} < 6$ and even for $\varepsilon_{LJ} = 6$, 8 the mass of the largest detached micelle is significantly smaller than the total mass $M_{mic}^{max} = 160$ of available surfactant.

C. Shapes of the complex

In the case of complex formation we characterize the shape of the complex in terms of its matrix of inertia

$$\Theta_{\alpha\beta} = \frac{1}{M}\sum_{j\in C}\left(\mathbf{r}_j^2\delta_{\alpha\beta} - r_j^{(\alpha)}r_j^{(\beta)}\right) \equiv \overline{r^2\delta_{\alpha\beta} - r^{(\alpha)}r^{(\beta)}} \tag{5}$$

where the sum is over all M beads j that are part of the complex and $r_j = (r_j^{(1)}, r_j^{(2)}, r_j^{(3)})$ is the position of bead j with respect to the center of mass of the complex. Diagonalizing $\Theta_{\alpha\beta}$ results in the three eigenvalues $\vartheta_x \geq \vartheta_y \geq \vartheta_z$ with respective axes x, y, z of the principal moments of inertia with the center of mass as the origin. Note that in these coordinates one has *e.g.*

$$\vartheta_z = \overline{x^2 + y^2} \tag{6}$$

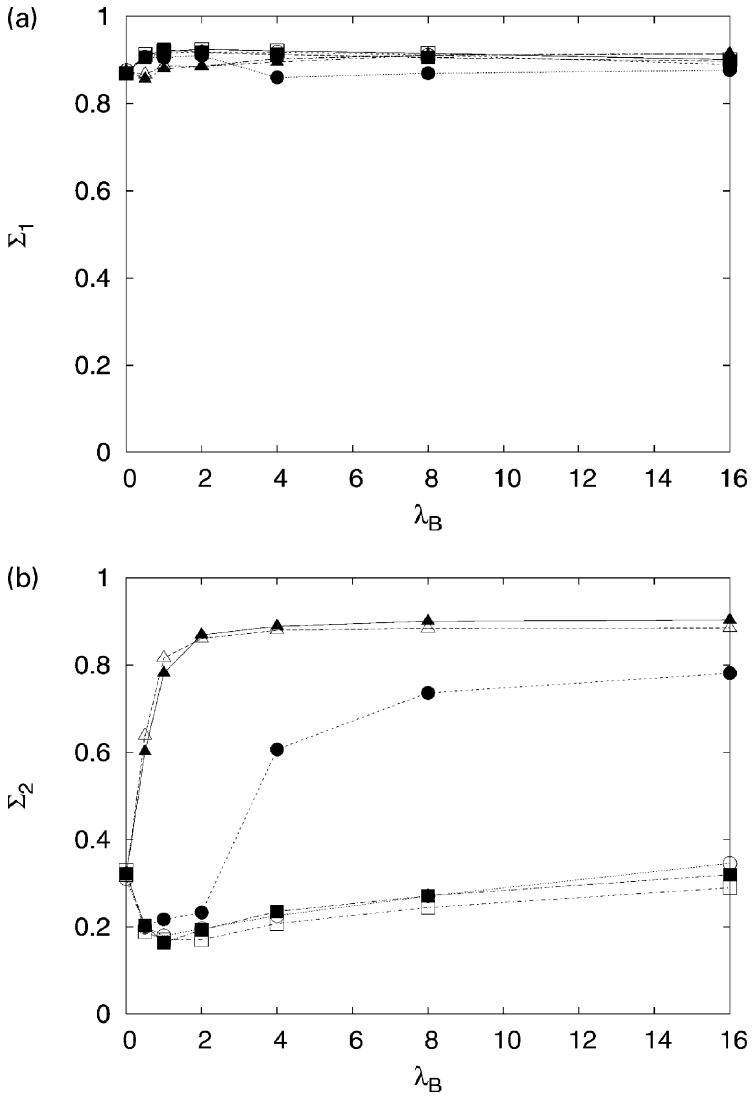

Fig. 7 (a) The ratio $\Sigma_1 = \vartheta_y/\vartheta_x$ of the second largest and largest principal moments of inertia and (b) the ratio $\Sigma_2 = \vartheta_z/\vartheta_x$ of the smallest and the largest principal moments of inertia as function of the Coulomb strength λ_B for different values of the hydrophobicity parameter $\varepsilon_{LJ} = 0(\square)$, $1(\blacksquare)$, $2(\bigcirc)$, $4(\bullet)$, $6(\triangle)$, $8(\blacktriangle)$ from below.

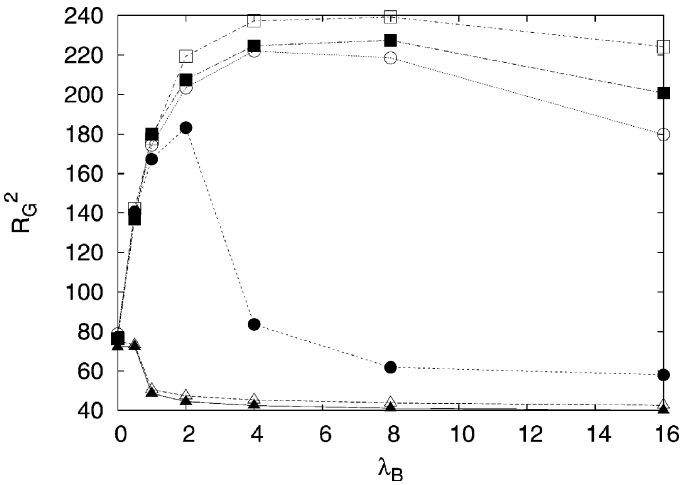

Fig. 8 The radius of gyration of the complex as a function of the Coulomb strength λ_B for different values of the hydrophobicity parameter $\varepsilon_{LJ} = 0(\square)$, $1(\blacksquare)$, $2(\bigcirc)$, $4(\bullet)$, $6(\triangle)$, $8(\blacktriangle)$ from above.

such that the radius R_G of gyration of the complex is given by

$$R_G^2 = \left(\vartheta_x + \vartheta_y + \vartheta_z\right)/2 = \tfrac{1}{2}\mathrm{Tr}\Theta$$

The relative values of the principal moments determine the global shape of the complex. The averaged ratios $\Sigma_1 = \langle\vartheta_y/\vartheta_x\rangle$ and $\Sigma_2 = \langle\vartheta_z/\vartheta_x\rangle$ are plotted as functions of the Coulomb strength λ_B for different hydrophobicities ε_{LJ} in Fig. 7. These serve as indicators for the transition of the complex from a cylindrical shape to an almost spherical one. The cylindrical shape is characterized by two large approximately equal inertia, *i.e.* $\Sigma_1 \approx 1$ and a third smaller moment such that $\Sigma_2 \approx 0.2\ldots0.3$. For an elongated cylindrical shape the z-axis corresponding to the smallest moment ϑ_z is the symmetry axis. The spherical shapes in turn are characterized by three almost equal moments of inertia with $\Sigma_2 \approx \Sigma_1 \approx 1$. We observe the following—see Fig. 7: At $\lambda_B = 0$, $\varepsilon_{LJ} = 0$ only the PE chain is part of the 'complex'. The corresponding values we find for the neutral chain are $\Sigma_1 = \langle\vartheta_y/\vartheta_x\rangle = 0.87$ and $\Sigma_2 = \langle\vartheta_z/\vartheta_x\rangle = 0.34$. These may be compared with $\langle\vartheta_y\rangle/\langle\vartheta_x\rangle = 0.87$ and $\langle\vartheta_z\rangle/\langle\vartheta_x\rangle = 0.27$ calculated from data found for self avoiding walks.[69] Note that the relation $\langle\vartheta_z/\vartheta_x\rangle > \langle\vartheta_z\rangle/\langle\vartheta_x\rangle$ is in accordance with the Schwartz inequality for averages. For weak hydrophobicity $\varepsilon_{LJ} < 3$ the shape of the complex remains cylindrical even for high Coulomb strength, while for strong hydrophobicity $\varepsilon_{LJ} > 5$ the transition from cylindrical to spherical shape occurs already for small Coulomb strengths $\lambda_B \approx 1$. For the intermediate hydrophobicity $\lambda_B = 4$ though, we observe a competition between the formation of the cylindrical bottle brush and the spherical micellar complex. This fact is expressed by the non-monotonic behavior of the shape parameter Σ_2 as a function of λ_B. While for small λ_B the cylindrical shape wins and Σ_2 decreases with respect to the value of the neutral situation, a transition occurs between $\lambda_B = 2$ and $\lambda_B = 4$ where the shape parameter indicates a transition towards the spherical micellar complex, with Σ_2 increasing to 0.6 and further towards 0.8 for $\lambda_B > 8$. To verify the transition we analyze the internal structure of these intermediate states in more detail below. A similar division into strong, weak and intermediate hydrophobicity we find for the behavior of the square radius of gyration R_G^2 which is plotted as function of λ_B in Fig. 8. For small hydrophobicity $\varepsilon_{LJ} < 3$ the behavior of R_G^2 parallels that of the square end-to-end distance R^2 as described above for the case $\varepsilon_{LJ} = 0$. For high hydrophobicity $\varepsilon_{LJ} > 5$ the radius of gyration of the complex shrinks already for small $\lambda_B \approx 1$ to values corresponding to compact micellar complexes. Again, the intermediate case $\varepsilon_{LJ} = 4$ behaves in a special way: For small Coulomb strengths $\lambda_B < 3$ the radius grows due to the stretching of the polyelectrolyte chain and only for higher $\lambda_B > 6$ it again shrinks below the polymer coil value but still remains well separated from the high hydrophobicity case.

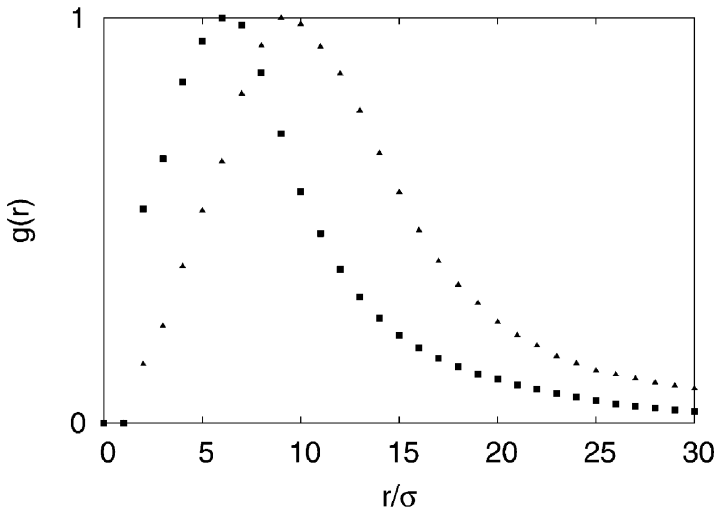

Fig. 9 The pair correlation function $g(r)$ for pairs of a polyelectrolyte monomer and a surfactant tail monomer at Bjerrum length $\lambda_B = 8\sigma$. The functions are scaled to a maximum value of 1. The maximal number of tail ends is found at $r = 6\sigma$ from the polyelectrolyte backbone in the case of $n = 5$(■) monomer surfactants. For $n = 10$(▲) this most probable distance is $r = 9\sigma$.

D. Internal structure of the complex

While the overall shape of the complex is characterized by the inertia matrix, its internal structure can be explored by either the internal monomer–monomer correlations or by the density distributions of the different complexes in a given reference frame. We have used both approaches to identify the key features of the self-assembled structures. To verify the idea of the molecular bottle brush like structures in the case of low hydrophobicity ε_{LJ} and high Coulomb strength λ_B, we have measured in particular the correlation between the polyelectrolyte monomers and the surfactant tail ends. As shown in Fig. 9 using also data from ref. 16 we indeed find that the surfactant tail end is found in this situation with highest probability at a distance from the polyelectrolyte chain that increases with the length of the tail in accordance with the bottle brush picture. To monitor, on the other hand, the internal reorganization along with the transition from the cylindrical bottle-brush to the spherical micellar aggregate, we chose as a reference frame a coordinate system defined by the directions of the principle moments of inertia of the complex with the origin at its center of mass. We define the x, y, z-directions such that the corresponding moments are ordered by $\vartheta_x \geq \vartheta_y \geq \vartheta_z$. As mentioned above, the z-axis then is the symmetry axis for the averaged cylindrical structures.

In Figs. 10–12 we show as examples for typical conformations of the complex the density distributions measured in this coordinate system. For vanishing hydrophobicity $\varepsilon_{LJ} = 0$ and $\lambda_B = 4$ the corresponding distributions are shown in Fig. 10. The densities as a function of the distance r_{xy} from the z-axis as plotted in Fig. 10(a) show clearly that the polyelectrolyte monomers and the surfactant heads are localized near the symmetry (z)-axis while the density of the surfactant-tail monomers surpasses that of the former two species at larger distances from the central axis. The distributions measured along the z-axis on the other hand show the remarkable feature of maxima near the ends of the cylinder. Surprising as it may seem, this effect is even exhibited by the equilibrium coil of a neutral polymer chain and in particular in our simulation for vanishing interactions.

The spherical micellar complexes, on the other hand, which we observe for sufficiently large parameter values of λ_B and ε_{LJ} are characterized by density distributions along and perpendicular to the z-axis that are nearly identical—see Fig. 11. Only the different differential volumes used for measurement lead to deviations. A more natural variable in the spherical case is of course the distance r from the center of mass. The density $\rho(r)$ as displayed in Fig. 11 parallels the corresponding results of Wallin and Linse obtained by a self-consistent spherical lattice field approach:[17] The core of the micelle is formed by almost densely packed surfactant tails surrounded

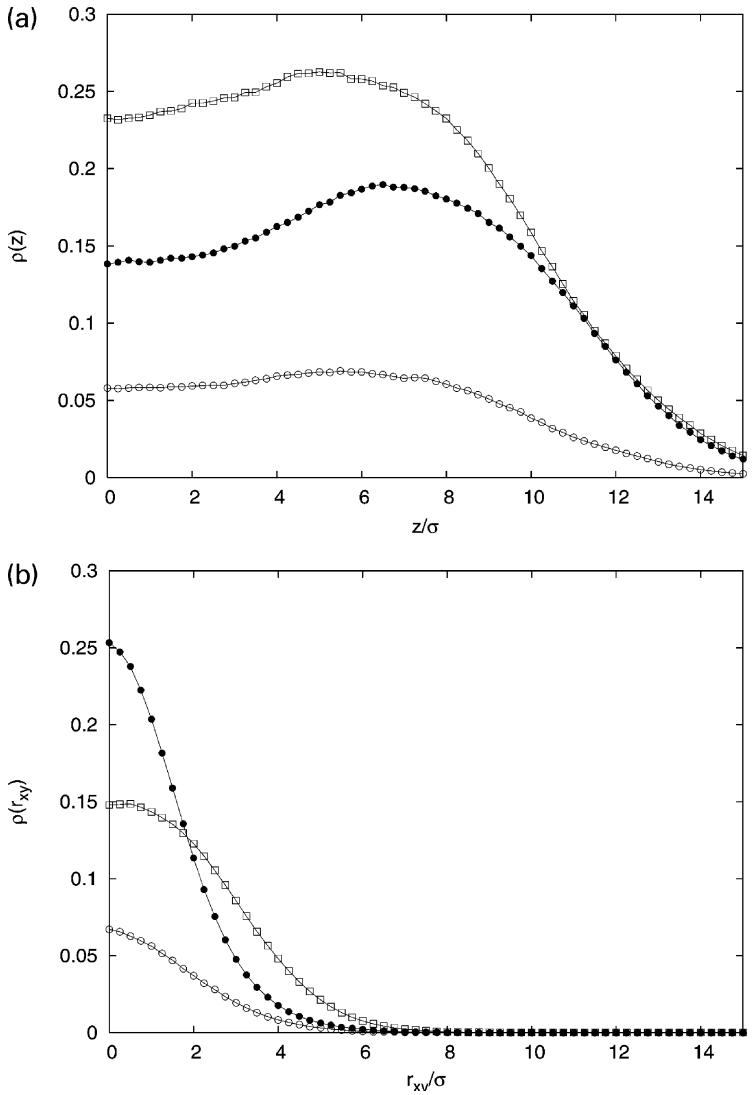

Fig. 10 Density distributions of monomers in directions (a) along the z-axis and (b) perpendicular to the z-axis for $\lambda_B = 0$, $\varepsilon_{LJ} = 4$ for polyelectrolyte beads (●), surfactant heads (○) and tail monomers (□).

by surfactant heads that stick out of the surface and another layer that contains the polyelectrolyte chain.

A transitional structure found for the values $\lambda_B = 4$ and $\varepsilon_{LJ} = 4$ of the interactions near to the boundary between the two states is investigated in Fig. 12. Although the structure is much more loosely bound it rather parallels the micellar aggregate displaying however a less pronounced layering in the spherical density distribution, see Fig. 12. The comparison of Fig. 12(a) and (b) however shows that the distributions display deviations from spherical symmetry. Nonetheless, the present data indicates that the transition between the two states of the complex is rather sharp.

V. Conclusions

In extensive MC simulations we have investigated the behavior of a single polyelectrolyte chain that interacts with oppositely charged surfactant molecules taking into account both long range

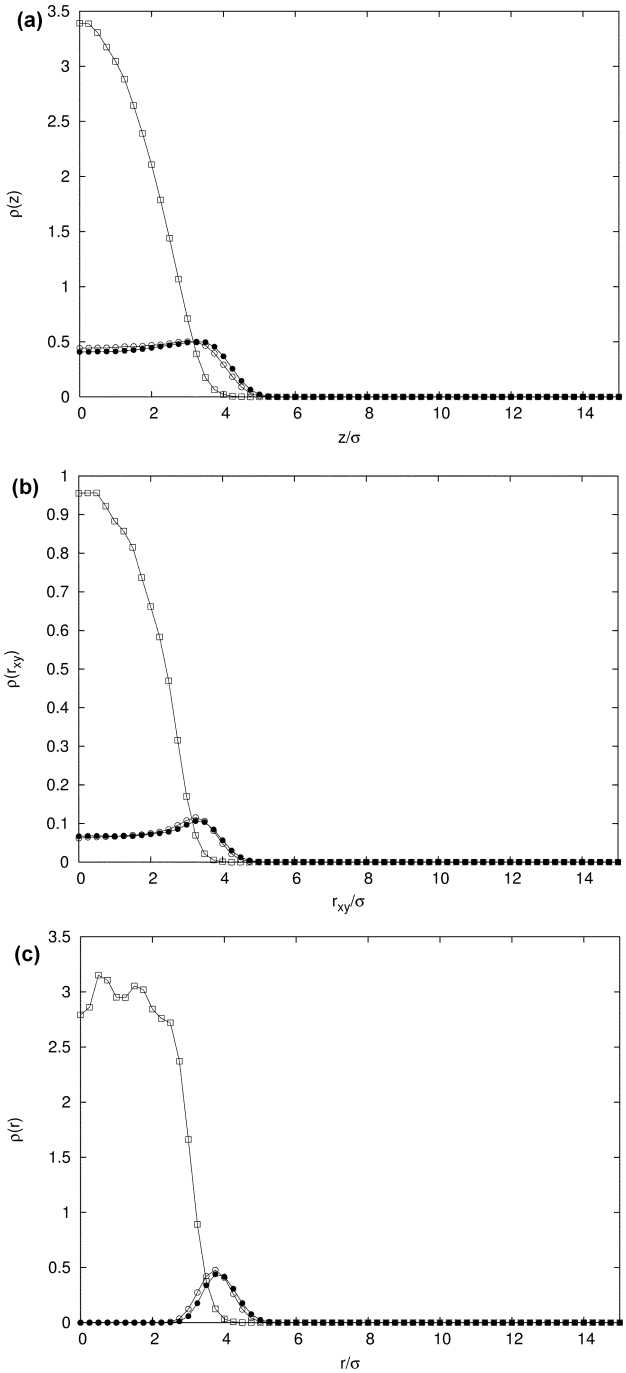

Fig. 11 Density distributions of monomers in directions (a) along the z-axis, (b) perpendicular to the z-axis, and (c) as function of the distance from the center of mass for $\lambda_B = 16$, $\varepsilon_{LJ} = 8$ for polyelectrolyte beads (●), surfactant heads (○) and tail monomers (□).

Coulomb and short range hydrophobic interactions. Exploring the parameter space in both of these interactions we have established a "phase diagram" for this system and several distinct regions ("phases") with characteristic structural behavior of the system as sketched in Fig. 1: for weak

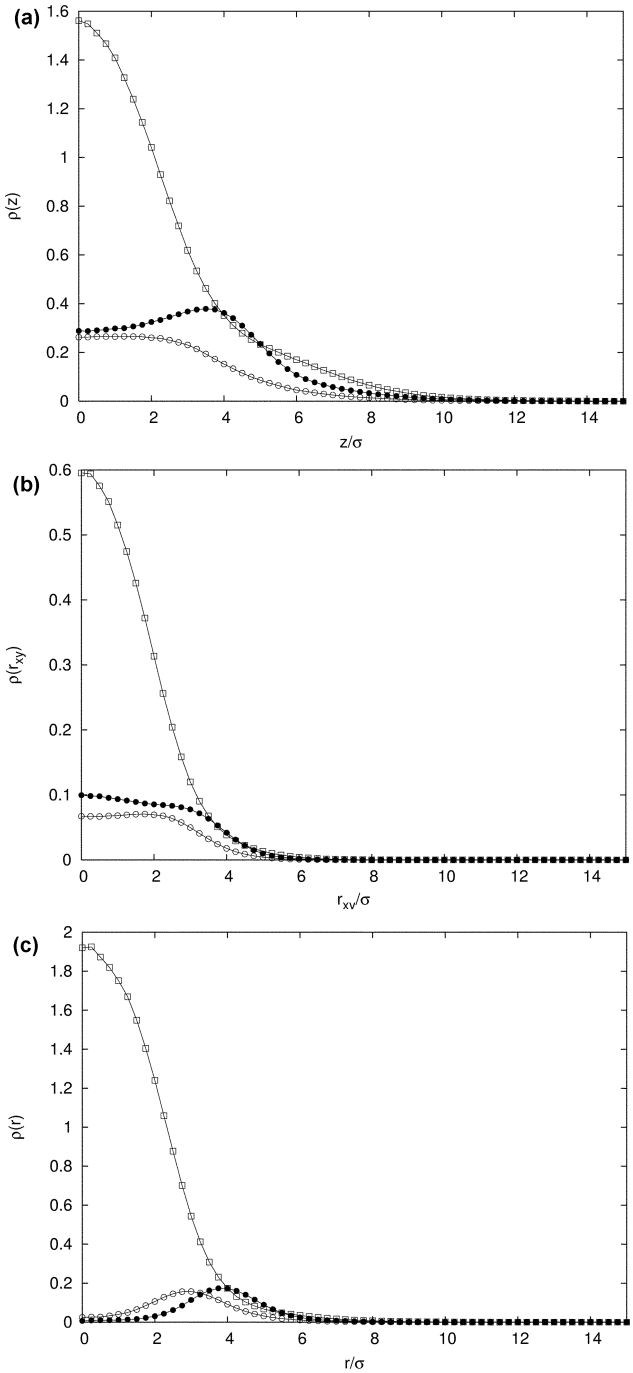

Fig. 12 Density distributions of monomers in directions (a) along the z-axis, (b) perpendicular to the z-axis, and (c) as function of the distance from the center of mass for $\lambda_B = 4$, $\varepsilon_{LJ} = 4$ for polyelectrolyte beads (●), surfactant heads (○) and tail monomers (□).

interactions both constituents behave nearly independently and the PE chain has a possibly stretched coil conformation. For high Coulomb strength but weak hydrophobicity we observe the formation of a complex with a cylindrical bottle brush structure in which the PE chain is

stretched along the cylinder axis. If both interactions are strong, an inverted spherical micellar complex structure emerges with the SF tails constituting the core of a spherical micelle and the SF heads and the PE chain confined to the surface of this sphere. For intermediate values of the hydrophobicity there is a competition between the two structurally different complexation modes resulting in a non-trivial behavior of the shape as function of the Coulomb strength. For high hydrophobicity, but low Coulomb interaction the surfactant forms micelles to which the PE chain is only loosely attached. As we have reported in ref. 16 complexation in this system is in general weakened by the addition of salt. Our results can in principle be verified in experiments by systematically varying the surfactant tail hydrophobicity and the surfactant/polyelectrolyte charge and/or the dielectric permittivity of the solvent.

A number of extensions of our present approach are possible and would be interesting to follow. Of particular interest would be a study of a multi PE-chain system. For small numbers of chains a corresponding simulation appears to be feasible using our present approach. One might expect to observe in such a case a competition between the cooperative assembly of a multichain complex and single chain complexation. At high densities in systems with many chains one expects the formation of layered structures with many different possible phases.[70] However, high density and a large number of chains are out of reach of the present approach, due to the requirement of calculating the long range interaction between any pair of charged beads and the slowing down of the simulation by the caging effect at high densities. To simulate such systems either one has to release the hard sphere non-penetrability[71] or resort to lattice methods and simulate only with a screened shorter range Coulomb interaction.

Other situations that can lead to significant changes in the behavior might be found for a choice of different valency of the SF heads and the PE chains to study over-charging effects of the polyelectrolyte for high valency salt ions.[72] Also, in general, introducing neutral beads to the PE chain and varying the distribution of charges along the chain may lead to significant effects. In addition, the chain stiffness has been shown to be an important parameter. For a single micelle modeled as a charged sphere, many recent studies have revealed different topologies of the defect depending on the chain stiffness.[26,32–46]

Appendix

A crude argument for the stability of micelles built from our model surfactants can be derived from the following considerations: We assume that the core of a spherical micelle is given by m_t tail monomers at a packing fraction η such that the core radius r_C is given by

$$r_C(m_t) = \frac{\sigma}{2}\left(\frac{m_t}{\eta}\right)^{1/3}. \tag{7}$$

The number of beads in the surface layer is then given by

$$m_\sigma(m_t) = \left[r_C^3(m_t) - \left(r_C(m_t) - \frac{\sigma}{2}\right)^3\right]\eta. \tag{8}$$

Assuming that each bead inside the core has 12 neighbors at an optimal distance (*i.e.* at the minimum of the potential V_{LJ}), while the surface beads have only 6 neighbors we find the total Lennard-Jones energy of the micelle as

$$\frac{1}{k_B T} E_{LJ}(m_t) = -(m_t - m_\sigma(m_t)/2)\frac{3}{2}\varepsilon_{LJ}. \tag{9}$$

The total Coulomb energy of the SF heads distributed on the micellar surface may be derived from the numerical solution of the Thomson problem for distributing k charges on a spherical surface which is given by the fit formula[73]

$$\frac{1}{k_B T} E_C(k, m_t) = \frac{\lambda_B}{r_C(m_t)}\frac{k^2}{2}\left(1 - ak^{-1/2} + bk^{-3/2}\right), \tag{10}$$

with $a = 1.10461$ and $b = 0.137$. Finally, we may estimate the relevant entropy term by assuming that for every molecule it is given by restricting it to the volume of the micelle. This volume entropy

term is thus

$$\frac{1}{k_B}S(k,m_t) = k\ln\left(r(m_t)^3\Big/\Omega\right) \tag{11}$$

where Ω is the total system volume. For our system of 32 surfactant molecules with one charged bead and four tail beads we have $m_t = 4k$ and a minimum of the free energy $F(k, m_t)$ with

$$\frac{1}{k_B T}F(k,m_t) = E_C(k,m_t) + E_{LJ}(m_t) - S(k,m_t) \tag{12}$$

at $n \neq 0$ existing for a given Coulomb interaction only for sufficiently large hydrophobicity. Note, however that our estimate is too crude to give more than an order of magnitude result showing that ε_{LJ} should be at least of the order of λ_B and of the order of $\varepsilon_{LJ} \sim 1$ for $\lambda_B = 0$ to find micellar aggregation for our case of surfactant length $n = 5$, *i.e.* $m_t = 4k$ and the given overall number of surfactant molecules $k \leq 32$.

Acknowledgements

We thank A. F. Thünemann, O. Farago, H. Diamant and R. Messina for helpful discussions. This work was supported by the Deutsche Forschungsgemeinschaft through grant No. LO 418/7.

References

1 J. C. T. Kwak, *Polymer-Surfactant Systems*, Marcel Dekker, New York, 1998.
2 M. Antonietti, C. Burger and A. Thünemann, *Trends Polym. Sci.*, 1997, **5**, 262.
3 P. Hansson and B. Lindman, *Curr. Opin. Colloid Interface Sci.*, 1996, **1**, 604.
4 E. Sokolov, F. Yeh, A. Khokhlov, V. Y. Grinberg and B. Chu, *J. Phys. Chem. B*, 1998, **102**, 7091.
5 S. Kosmella, J. Kotz, K. Shirahama and J. Liu, *J. Phys. Chem. B*, 1998, **102**, 6459.
6 P. M. Claesson, M. L. Fielden, A. Dedinaite, W. Brown and J. Fundin, *J. Phys. Chem. B*, 1998, **102**, 1270.
7 M. Tsianou and P. Alexandridis, *Langmuir*, 1999, **15**, 8105.
8 A. F. Thünemann, S. Kubowicz and U. Pietsch, *Langmuir*, 2000, **16**, 8562.
9 R. Dias, S. Mel'nikov, B. Lindman and M. G. Miguel, *Langmuir*, 2000, **16**, 9577.
10 V. G. Babak, E. A. Merkovich, J. Desbrieres and M. Rinaudo, *Polym. Bull.*, 2000, **45**, 77.
11 X. M. Liao and D. A. Higgins, *Langmuir*, 2001, **17**, 6051.
12 Y. Guan, Y. P. Cao, Y. X. Peng, J. Xu and A. S. C. Chen, *Chem. Commun.*, 2001, **17**, 1694.
13 D. J. F. Taylor and R. K. Thomas, *Langmuir*, 2002, **18**, 4748.
14 P. Hansson, S. Schneider and B. Lindman, *J. Chem. Phys. B*, 2002, **106**, 9777.
15 S. Guillot, D. M. Loughlin, N. Jain, M. Delsanti and D. Langevin, *J. Phys.: Condensed Matter*, 2003 **15**, S219.
16 C. von Ferber and H. Löwen, *J. Chem. Phys.*, 2003, **118**, 10 774.
17 T. Wallin and P. Linse, *Langmuir*, 1998, **14**, 2940.
18 K. Shirahama, H. Yuasa and S. Sugimoto, *Bull. Chem. Soc. Jpn.*, 1981, **54**, 375.
19 K. Shirahama and M. Tashiro, *Bull. Chem. Soc. Jpn.*, 1984, **57**, 377.
20 R. Sear, *J. Phys.: Condensed Matter*, 1998, **10**, 1677.
21 P. S. Kuhn, Y. Levin and M. C. Barbosa, *Chem. Phys. Lett.*, 1998, **298**, 51.
22 P. S. Kuhn, M. C. Barbosa and Y. Levin, *Physica A*, 2000, **283**, 113.
23 M. B. A. Silva, P. S. Kuhn and L. S. Lucena, *Physica A*, 2001, **296**, 31.
24 H. Diamant and D. Andelman, *Phys. Rev. E*, 2000, **61**, 6740.
25 H. Diamant and D. Andelman, *Macromolecules*, 2000, **33**, 8050.
26 T. Wallin and P. Linse, *Langmuir*, 1996, **12**, 305.
27 M. Stevens and K. Kremer, *J. Chem. Phys.*, 1995, **103**, 1669.
28 R. G. Winkler, M. Gold and P. Reineker, *Phys. Rev. Lett.*, 1998, **80**, 3731.
29 U. Micka, C. Holm and K. Kremer, *Langmuir*, 1999, **15**, 4033.
30 N. V. Brilliantov, D.V. Kuznetsov and R. Klein, *Phys. Rev. Lett.*, 1998, **81**, 1433.
31 P. S. Kuhn, *Physica A*, 2002, **311**, 50.
32 E. Gurovitch and P. Sens, *Phys. Rev. Lett.*, 1999, **82**, 339.
33 E. Mateescu, C. Jeppesen and P. Pincus, *Europhys. Lett.*, 1999, **46**, 493.
34 R. R. Netz and J.-F. Joanny, *Macromolecules*, 1999, **32**, 9026.
35 S. Y. Park, R. F. Bruinsma and W. M. Gelbart, *Europhys. Lett.*, 1999, **46**, 454.
36 K. K. Kunze and R. R. Netz, *Phys. Rev. Lett.*, 2000, **85**, 4389.
37 T. T. Nguyen and B. I. Shklovskii, *Physica A*, 2000, **293**, 324.

38 P. Welch and M. Muthukumar, *Macromolecules*, 2000, **33**, 6159.
39 H. Schiessel, R. F. Bruinsma and W. M. Gelbart, *J. Chem. Phys.*, 2001, **115**, 7245.
40 M. Jonsson and P. Linse, *J. Chem. Phys.*, 2001, **115**, 3406.
41 M. Jonsson and P. Linse, *J. Chem. Phys.*, 2001, **115**, 10 975.
42 A. Akinchina and P. Linse, *Macromolecules*, 2002, **35**, 5183.
43 P. Chodanowski and S. Stoll, *J. Chem. Phys.*, 2001, **115**, 4951.
44 P. Chodanowski and S. Stoll, *Macromolecules*, 2001, **34**, 2320.
45 M. Brynda, P. Chodanowski and S. Stoll, *Colloid Polym. Sci.*, 2002, **280**, 789.
46 K. Keren, Y. Soen, G. B. Yoseph, R. Gilad, E. Braun, U. Silvan and Y. Talmon, *Phys. Rev. Lett.*, 2002 **89**, 88 103.
47 G. ten Brinke and O. Ikkala, *Trends Polym. Sci.*, 1997, **5**, 213.
48 J. Ruokolainen, G. ten Brinke, O. Ikkala, M. Torkkeli and R. Serimaa, *Macromolecules*, 1996, **29**, 3409.
49 T. M. Birshtein, O. V. Borisov, Y. B. Zhulina, A. R. Khokhlov and T. A. Yurasova, *Polym. Sci. USSR*, 1987, **29**, 1293.
50 G. H. Fredrickson, *Macromolecules*, 1993, **26**, 2825.
51 Y. Rouault and O. V. Borisov, *Macromolecules*, 1996, **29**, 2605.
52 P. G. Khalatur, D. G. Shirvanyanz, N. Y. Starovoitova and A. R. Khokhlov, *Macromol. Theory Simul.*, 2000, **9**, 141.
53 J.-P. Hansen and H. Löwen, *Annu. Rev. Phys. Chem.*, 2000, **51**, 209.
54 R. D. Groot, *Langmuir*, 2000, **16**, 7493.
55 J. Rescic and P. Linse, *J. Phys. Chem. B*, 2000, **104**, 7852.
56 T. Wallin and P. Linse, *J. Phys. Chem. B*, 1997, **101**, 5506.
57 R. G. Winkler, M. O. Steinhauser and P. Reineker, *Phys. Rev. E*, 2002, **66**, 21 802.
58 A. Jusufi, C. N. Likos and H. Löwen, *Phys. Rev. Lett.*, 2002, **88**, 18 301.
59 R. Messina, C. Holm and K. Kremer, *Phys. Rev. E*, 2002, **65**, 41 805.
60 T. Odijk, *Macromolecules*, 1979, **12**, 688.
61 M. Fixman and J. Skolnik, *Macromolecules*, 1978, **11**, 863.
62 P. G. deGennes, P. Pincus and R. Velasco, *J. Phys. (Paris)*, 1976, **37**, 1461.
63 J.-L. Barrat and J.-F. Joanny, *Europhys. Lett.*, 1993, **3**, 343.
64 R. Connolly, E. G. Timoshenko and Y. A. Kuznetsov, *J. Chem. Phys.*, 2003, **119**, 8736.
65 E. G. Timoshenko and Y. A. Kuznetsov, *J. Chem. Phys.*, 2000, **112**, 8163.
66 J. Lekner, *Physica A*, 1991, **176**, 485.
67 H. Schiessel and P. Pincus, *Macromolecules*, 1998, **31**, 7953.
68 M. Doi and S. F. Edwards, *The Theory of Polymer Dynamics*, Oxford University Press, Oxford, 1986.
69 G. Zifferer, *J. Chem. Phys.*, 1998, **109**, 3691.
70 A. Thünemann, *Langmuir*, 1997, **13**, 6040.
71 R. D. Groot, *J. Chem. Phys.*, 2003, **118**, 11 265.
72 R. Messina, C. Holm and K. Kremer, *J. Chem. Phys.*, 2002, **117**, 2947.
73 J. R. Morris, D. M. Deaven and K. M. Ho, *Phys. Rev. B*, 1996, **53**, R1740.